Experimental Characterization of Crack Sensitivity under Continuous Casting Conditions

C. Bernhard[*)], R. Pierer[*)], A. Tubikanec[*)], C.M. Chimani[**)]
[*)] Christian Doppler Laboratory for Metallurgical Fundamentals of Continuous Casting Processes (MCC), Department of Metallurgy, University of Leoben, Austria
[**)] VOEST-ALPINE Industrieanlagenbau GmbH, Linz, Austria

INTRODUCTION

There has been a constant increase in expert knowledge of the interaction between casting process, material properties, microstructure and crack sensitivity. The potential of numerical simulation has increased and there has been enormous technological progress. However, the formation of defects is still an economic problem in continuous casting.

In continuous casting the solidifying strand shell experiences both mechanical and thermal loads resulting from:

- contraction and phase transformation;
- temperature gradients along the surface or across the shell;
- friction between strand and mold;
- bending and straightening;
- bulging;
- soft reduction etc.

These loads act on the material, which is more or less crack sensitive within certain critical temperature ranges depending on the steel composition and the

- enrichment of segregating elements and/or formation of low melting phases between dendrites or grain boundaries,
- precipitation of oxy-sulfides, nitrides and carbonitrides,
- formation of proeutectoid ferrite along austenite grain boundaries.

These critical temperature ranges are often termed the brittle temperature ranges: BTR I and BTR II. In common hot tearing criterions, the critical limits for shell deformation are often connected with BTR I. One of these criterions was proposed by Won et al.[4]. **Figure 1** shows experimentally determined critical strain values versus equivalent carbon content C_{equ}, together with the calculated critical strain from Won´s model for the testing conditions of Matsumyia[1]. As can be seen, the model considers the influence of microsegregation on BTR I (here termed ΔT_B), and hence, the influence of the alloying elements. Increasing strain rate $\dot{\varepsilon}$ lowers the critical strain ε_c. φ, n and m are fitting parameters. This quite simple approach allows the calculation of ε_c over a wide range of compositions and testing conditions, in good correspondence with the reported values, as can be seen in **Figure 2**. The influence of steel composition and strain rate on crack susceptibility within BTR I can thus be quantified, but there are other influencing parameters, much more difficult to consider.

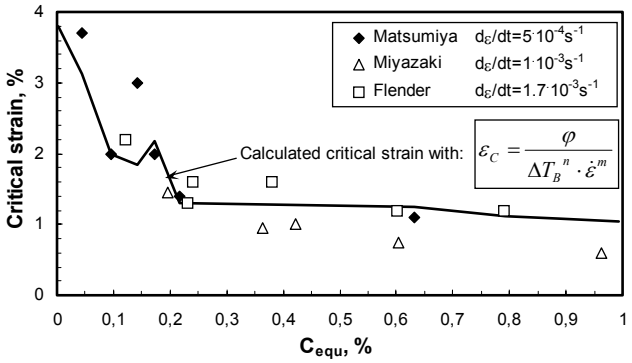

Figure 1: Experimentally measured critical strain[1-3] for crack formation in BTR I and calculated values[4] over the C_{equ}

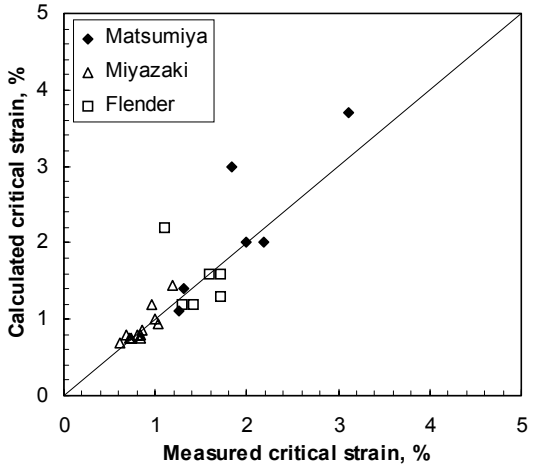

Figure 2: Comparison of calculated critical strain for crack formation with experimentally measured data[1-3]

At higher temperatures, the mechanical properties of the strand shell depend on the (micro)structure of the solidifying material, the formation of precipitates or the existence of harmful phases. The influence of these parameters has not only to be considered in numerical models, but also in experimental simulation.

Crystallization perpendicular to the direction of heat extraction generates a highly anisotropic structure with unfavorable orientation of weak regions caused by e.g. interdendritic voids and grain boundaries perpendicular to the main load directions. These microscopic inhomogeneities can trigger the local damage mechanism and a distinctly anisotropic crack susceptibility of the cast material is evident.

A laboratory method for the simulation of crack formation in continuous casting must therefore take into account several aspects:

- the microstructure of the solidifying shell by adjusting of the cooling conditions in the simulated process;
- the fact that the main load directions are perpendicular to the main dendrite growth axis;
- the existence of a deformable mushy zone in order to simulate crack formation in BTR I;
- an anisotropic grain structure, not reheated or normalized, with precipitation and proeutectoid ferrite formation along austenite grain boundaries (BTR II).

Most of these demands have been realized in the submerged split-chill tensile (SSCT) test, a proven laboratory method for the characterization of thermal contraction, tensile forces and crack sensitivity in the first ductility minimum. The results of these tests are the basis of a current joint VAI - MCC project on internal crack formation in higher carbon steels.

A new modification of the testing procedure now allows contraction and tensile tests to be performed at lower temperatures, and provides data on crack sensitivity within the second ductility trough.

In this paper, some background information on the test method and results from both projects are presented together with conclusions and future perspectives.

EXPERIMENTAL

The SSCT test

Figure 3 shows a schematic view of the SSCT test method[5-10]. A solid steel test body, split in two halves, is submerged into the liquid melt in an induction furnace. The surface of the test body is spray-coated with a thin zirconium oxide layer in order to control the cooling conditions and to minimize friction. A steel shell solidifies around the test body with the main crystallographic orientation perpendicular to the interface, similar to the situation in a continuous casting mould. The force between the upper and lower parts of the test dummy is measured by a load cell, the position of the lower part by an inductive position sensor. A servo-hydraulic controller controls forces and position.

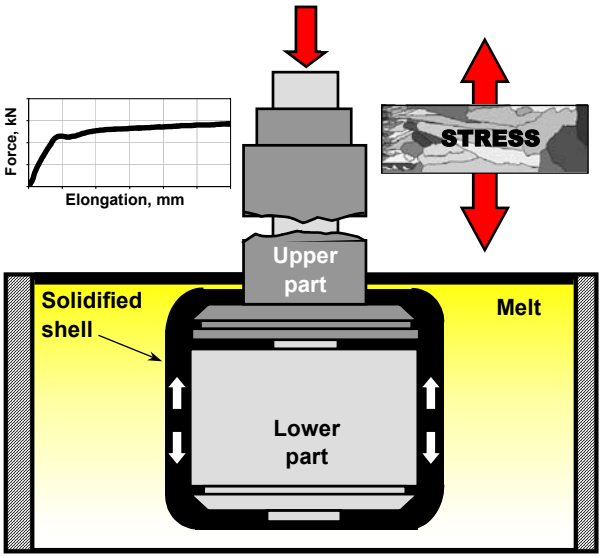

Figure 3: SSCT test method, schematic

This allows a number of different testing procedures.

- Hot tensile test: after a certain holding time, the lower part of the test body is moved downwards at a controlled velocity at strain rates typically between 10^{-3} and 10^{-2} s^{-1}. The tensile force is recorded.
- Contraction force test: the lower part of the test body remains in its original position, the resulting force, proportional to the contraction force, is recorded.
- Contraction test: after initial solidification the shell is pre-loaded with a marginal load, the lower part moves upwards under the contraction force of the solidifying shell.

Each of these testing procedures takes place inside the induction furnace, preventing direct observation. The interpretation of results therefore requires the numerical simulation of solidification based on the temperatures measured. An inverse model allows the calculation of heat transfer

coefficients from temperature measurements inside the test body. The numerical simulation determines shell thickness and temperature distribution across the solidifying shell during the test procedure.
After tensile testing, the test body and solidified shell are immediately removed from the melt. The cooled specimens are cut and up to 16 metallographic specimens are prepared. The number, length and width of all detected cracks – classified according to characteristic types – are summarized in a crack index, allowing a quantitative indication of the deterioration of the shell dependent on the testing conditions.

In-situ material characterization test

For thermal reasons, the duration of an SSCT test is limited to approx. 30s. This restricts the shell/test body interface temperature (corresponding to the strand surface temperature) to temperatures just above 1000 °C. A new testing procedure was therefore developed in a co-operation between VAI and the University of Leoben. After a short solidification time inside the melt, the test body is removed from the melt and is allowed to cool in an inert gas atmosphere. The cooling rate is determined by the radiation condition and the atmosphere, resulting in cooling rates of the reported experiments. During solidification and cooling the servo-hydraulic control keeps the shell free from contraction forces in the axial direction. After cooling time of 20-30s, the mean temperature of the shell amounts to between 900 and 700 °C. At these typical temperature interval the ductility is significantly influenced by the start of pro-eutectoid ferrite formation and the precipitation of nitrides. The lower part of the test body is moved downwards at controlled velocity up to a strain of 0.1, exceeding the ultimate strain in most cases, or to the maximum available force of 45 kN.
This new procedure allows tensile tests on steel at temperatures in the BTR II. The microstructure and hence also the material properties of the specimen corresponds to the structure of a solidified strand shell, compare **Figure 4.** It should be mentioned that as a result of the relatively high cooling rate of the first test series reported hereafter, the precipitation of nitrides or carbo-nitrides might have been suppressed.

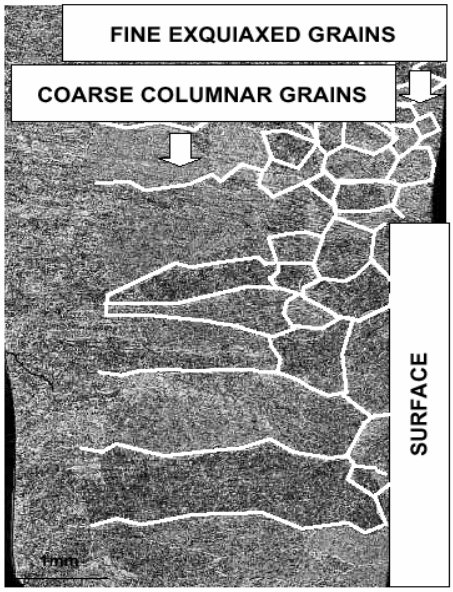

Figure 4: Anisotropic grain structure (austenite grain boundaries plotted in white) on the micrograph of a SSCT-test specimen

Numerical Simulation

In order to evaluate the stress and strain distribution within the test specimen, a fully coupled thermo-mechanical model of the SSCT-test has been developed on basis of the Finite Element (FE) method.
Figure 5 shows the axissymmetric model of the solid steel test body and the chosen mesh of the three domains, the upper and lower part of the test body and the steel melt. The mesh emploed axisymmetric 4 node continuum elements. In order to account for high level of stress – strain gradients at the interface between the test body and the melt, the mesh is locally refined.

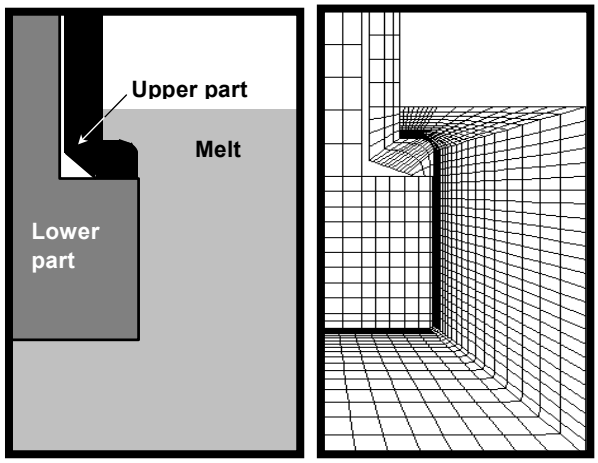

Figure 5: Finite Element model of the SSCT test (geometry and mesh)

To reduce computation time, the first analysis employed a rate-independent elasto-plastic material law based on standard Mises plasticity . The continuous improvement of the available high temperature material data for simulation purposes, as a result of adjustments to the experimental data of the SSCT-tests is one of the additional tasks of the actual project. The expected benefits are "near-process" material laws including rate dependent plasticity of a solidifying strand shell.

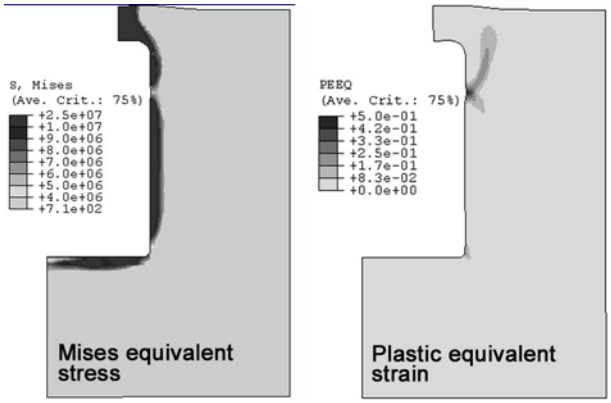

Figure 6: Results of equivalent stress and equivalent plastic strain in the solidified steel shell

Figure 6 shows equivalent plastic strain and the equivalent stress for a tensile test after 4s solidification time, strain rate $6 \cdot 10^{-3}$ s^{-1} and global strain of 0.016. The test conditions and results will be described in detail later. For these testing conditions, a local maximum equivalent strain arises in the shell between the upper and lower part of the test body, resulting in a total tearing of the shell in this region. This was confirmed by the metallografic examination of the test specimen. It should be mentioned, that longer solidification times and hence, thicker shells yield a more uniform strain distribution over the length of the specimen. The described FE-model visualizes the strain concentration on the macroscopic scale within the solidifying shell, and allows to quantify the relation between global and local strain. This is essential for the definition of critical strain limits.

RESULTS AND DISCUSSION

SSCT tests

The test series described here, with 12 hot tensile tests, was performed on steel of a constant composition (**Table 1**) under different testing conditions. For a zirconium oxide coating thicknesses of 0.15 and 0.4 mm the holding time was varied between 4, 8 and 12s, and the strain rate between $2 \cdot 10^{-3}$ and $6 \cdot 10^{-3}$ s^{-1}. The coating thickness of 0.15 mm corresponds to the cooling conditions in a typical bloom casting mold, a maximum heat flux of 2.4 MW/m², and a mean heat flux of 1.45 MW/m², whereas a coating thickness of 0.40 mm corresponds to a maximum heat flux of 1.7 MW/m² and a mean heat flux of 1.25 MW/m^2, i.e. to slab casting conditions.

	C	Si	Mn	P	S	Al
Aim	**0,18**	**0,25**	**1,4**	**0,01**	**0,01**	**0,045**
Min	0,16	0,2	1,3	0	0	0,02
Max	0,2	0,4	1,5	0,025	0,01	0,07

Table 1: Steel composition for SSCT-test

As outlined above, the measured temperature forms the basis of a solidification model. **Figure 7** shows the calculated shell growth vs. solidification time for the isotherms corresponding to solid fractions of 0, 0.5 and 1 together with the measured shell thickness after removal from the melt for a coating thickness of 0.4 mm. As it can be seen, the measured shell thickness corresponds with a calculated solid fraction of approx. 0.2. Hence the calculated results are in good agreement with the measured results, an important basis for the reliability of the test results, compare[9].

Figure 7: Calculated and measured shell

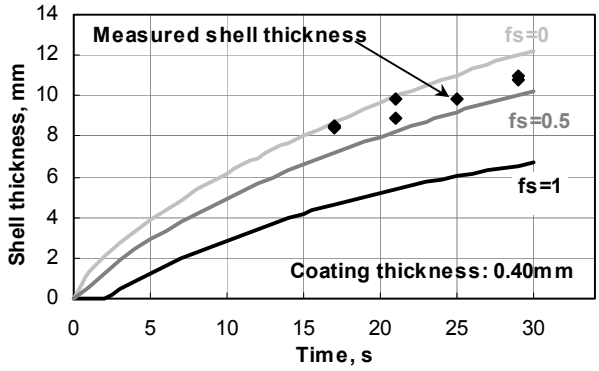

thickness for a coating thickness of 0.4 mm (low cooling rate)

Figures 8a and 8b show force-elongation curves for the tests at a coating thickness of 0.15 mm (3a) and 0.40 mm (3b), strain rate $6 \cdot 10^{-3}$ s^{-1}, and holding time of 4, 8 and 12 s. The tendency is as expected: increasing the holding time and therefore increasing the shell thickness and lowering the shell temperature leads to increasing tensile forces. The shape of the curve in Figure 3b for a holding time of only 4 s and a coating thick-

ness of 0.40 mm with a distinct maximum and subsequent decreasing tensile force indicates the occurrence of massive damage to the shell during testing.

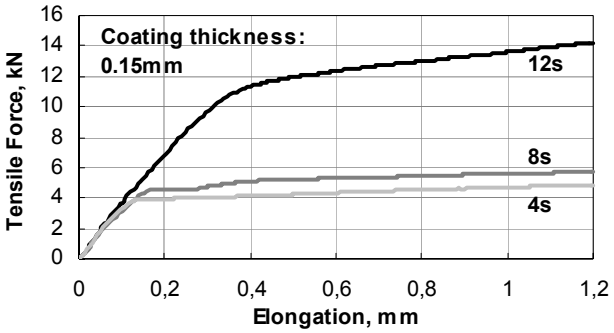

Figure 8a: Force-elongation curves for tests at the high cooling rate, strain rate $6 \cdot 10^{-3}$ s^{-1}, solidification time 4, 8, 12 s

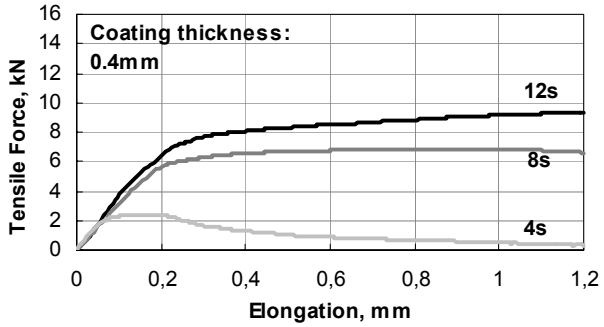

Figure 8b: Force-elongation curves for tests at the low cooling rate, strain rate $6 \cdot 10^{-3}$ s^{-1}, solidification time 4, 8, 12 s

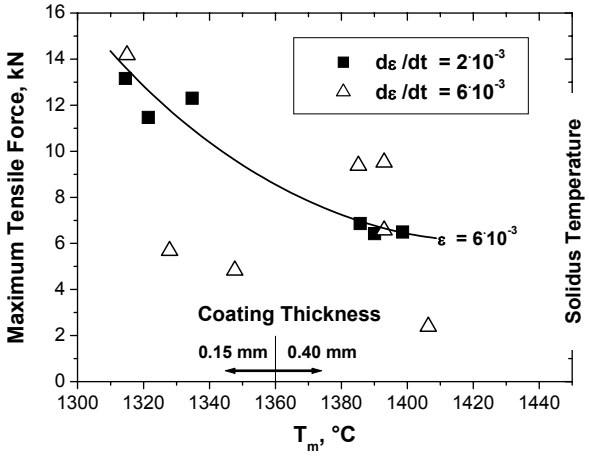

Figure 9: Maximum tensile forces measured over the mean shell temperature during testing

Figure 9 summarizes the maximum tensile forces measured over the mean temperature of the shell during testing. The values on the right are from the tests at the low cooling rate (0.40 mm coating thickness). The values on the left from the test series at higher cooling rates and comparatively lower mean testing temperature. A decrease in the mean shell temperature equates to an increase in holding time and an increase in shell thickness.

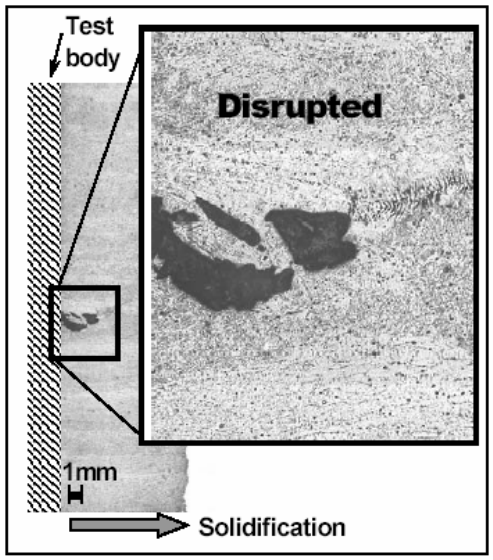

Figure 10a: Micrograph of specimen with disrupted shell: low cooling rate, strain rate $2 \cdot 10^{-3}$ s^{-1}, solidification time 4s

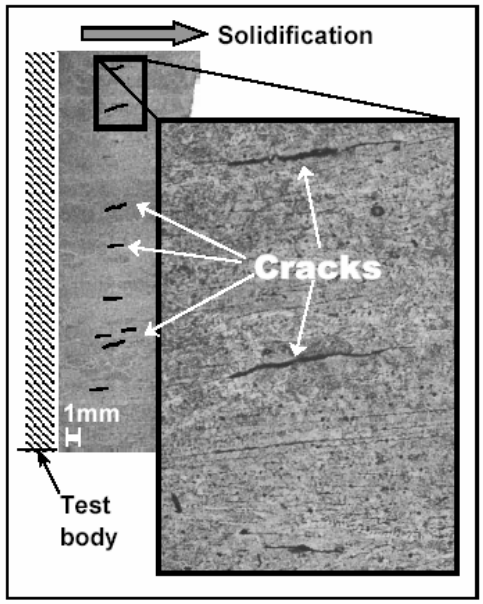

Figure 10b: Micrograph of specimen with cracks: high cooling rate, strain rate $6 \cdot 10^{-3}$ s^{-1}, solidification time 4s

The tendency towards increasing tensile force with decreasing temperature is obvious, but there are still differences between forces ascertained for similar testing conditions. The reason for these differences can be found in the metallographic examinations of the specimens.
An analysis of micrographs from 16 specimens for every test was carried out. **Figures 10a** and **10b** show micrographs of two test specimens tested at constant solidification time, but at different strain rates and cooling rates, which causes different degrees of deterioration. In Figure 10a a wide, open crack is visible. The shell deteriorated during the early stages of tensile testing, leading to a strain concentration within a very small area. The crack initiation site is interdendritic but the crack subsequently grew along grain boundaries. Specimens with such a heavily damaged shell are classified as “disrupted”.
In Figure 10b many interdendritic cracks, marked by white arrows, are visible over the whole length of the specimen. This indicates that the strain distribution at crack initiation is uniform along the interface direction in the shell. In **Figure 11** test specimens with interdendritic cracks, but with no tearing are classified as “cracks”. In some test specimens no cracks were found.

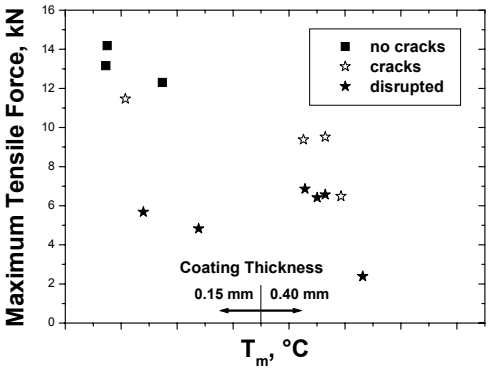

Figure 11: Classification of shell deterioration for the steels tested

Figure 11 summarizes the results of the metallographic examinations and the maximum tensile forces measured. As it can be seen, “disrupted speciments ” correspond to lower tensile forces than those specimens with cracks.
These first results indicate the dependence of the crack susceptibility on the test conditions. An applied strain of 0.024 does not necessarily result in the formation of cracks. The tests at the higher cooling rate, corresponding to a fine microstructure, are obviously less crack-sensitive. A higher strain rate results in more cracks at higher temperatures corresponding to lower tensile forces. If no cracks are formed, an increasing strain rate slightly increases the maximum tensile force.
In combination with the numerical analysis presented in the previous chapter this procedure is applied to evaluate the influence of the steel composition on the crack sensitivity in the BTR I

In-situ materials characterization test

The concept of the in-situ materials characterization test was realized in a joint research project between the CD-laboratory for functionally oriented materials design at the Vienna University of Technology, VAI and the Department of Metallurgy at Leoben University. The idea behind the concept is to expand the advantages of the SSCT test to temperatures below 1000 °C, necessary for material characterization at temperatures close to the austenite – ferrite transformation, considering the characteristics of a continuously cast microstructure.
For the reported experiments three different steel grades were used, **Table 2** gives the composition of the three tests on steel grade C.

Series C	C, %	Si, %	Mn, %	Nb, %
C1	0,173	0,4	1,6	0,026
C2	0,16	0,35	1,56	0,026
C3	0,155	0,42	1,58	0,024

Table 2: Composition of the three tests on steel C

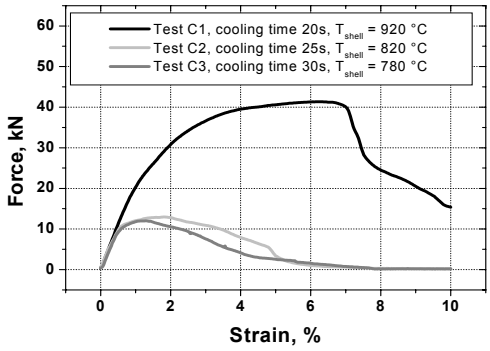

Figure 12: Force-elongation curves for steel grade C, cooling times 20, 25 and 30 s, strain rate $5 \cdot 10^{-3}$ s^{-1}, total strain 0.1

Figure 12 shows resulting force-elongation curves for steel grade C, a solidification time of 4 s and a cooling time of 20, 25 and 30 s, corresponding to shell mean temperatures of 920, 820 and 780 °C, respectively. The total tensile strain amounts to 0.1, strain rate $5 \cdot 10^{-3}$ s^{-1}. At 920 °C the tensile force reaches over 40 kN. Based on a shell thickness of approx. 4 mm, this corresponds to a maximum tensile stress of 60 MPa, which is significantly below data from literature for this steel grade in the temperature range between 800 and 900°C[11]. After reaching the ultimate tensile stress, the stress suddenly decreases as a result of massive crack formation in the specimen. Some parts of the shell are still connected, and therefore the stress does not decrease to zero.

Increasing the cooling time results in a lower specimen temperature and a radical worsening of the deformation capability: after reaching a maximum tensile force of around 13 kN, the shell tears and the remaining strength decreases to nearly zero. The same behavior can be obtained for a further decrease in temperature to 780 °C.

The strain to failure form these experiments evaluated from the given force – elongation curves is from 0.015 to 0.02. Typical values also experienced in the continuous casting process.

These results are in contrast to the well-known results of hot tensile tests where a decreasing ductility does not necessarily result in decreasing tensile strength and the critical strain levels leading to material failure are typically one order of magnitude higher.

It is assumed that this result is a consequence of the anisotropic casting structure and additionally the onset of pro-eutectoid ferrite formation. For conventional hot tensile tests the crystal structure is equiaxed and hence local disturbances like e.g. grain boundaries and precipitation have a minor influence on the material strength. It should be mentioned that the reported investigation method might lead to preexisting defects before the onset of the tensile test . The existence of these defects can not always be avoided, although the shell is kept free from contraction stresses in longitudinal direction circumferential contraction stresses can not be avoided. The pre-damaging of the shell has to be considered in the assessment of each test run. In case of heavy pre-damaging the test has to be excluded from evaluation.

Since the reported test runs are focused on the influence of Niobium, test conditions were chosen to avoid the formation of pro-eutectoid ferrite as a major reason for the formation of the second ductility trough. The cooling rate during testing is relatively high, as no measures were taken to reduce the heat removal. The proeutectoid ferrite formation is suppressed (calculated equilibrium ferrit formation temperature Ae3≈800°C) and the transformation is predicted to be bainite and martensite. These results are confirmed by metallography as shown in **Figure 13**.

The fracture surfaces were examined by electron microscopy at the Erich Schmid Institute of Materials Science at Leoben University and using light optical microscopy at the Department of Metallurgy. **Figure 13** shows an example for the micrograph (nital etch) of a ruptured shell. The crack has mainly interdendritic but also intergranular characteristics. Thus also the material failure appeared at temperatures, which are classical related to the BTR II (700-900°C) the interdendritic crack growth path would typically lead to the interpretation of BTR I failure mechanism, e.g. interdendritic crack growth at solid – liquid interface. In this case the most likely explanation to this observations is, that Nb as severely segregating element leads to the precipitation of (Ti,Nb)(C,N) during solidification at the dendrites boundaries. In consequence this precipitates trigger a localized material de-terioration leading to interdendritic crack growth also in the fully solidified state. The clarification and deeper understanding of these new insights are the aims of further work.

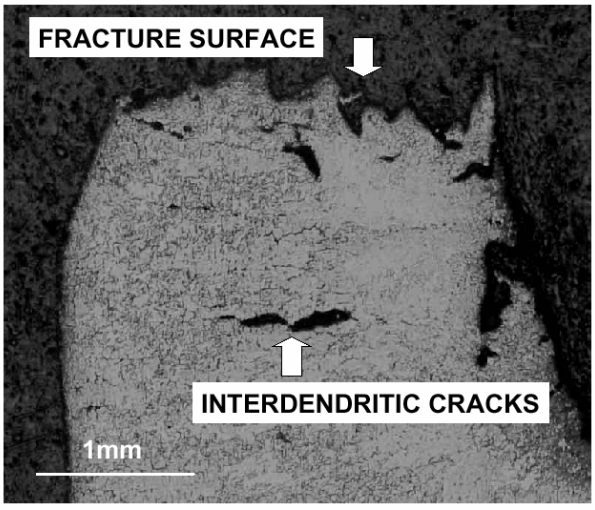

Figure 13: Micrograph perpendicular to the fracture surface, Bêchet-Beaujard etch

CONCLUSIONS AND OUTLOOK

The SSCT test is a proven method for the characterization of high temperature mechanical properties and the crack susceptibility of steel under continuous casting conditions. By considering the process parameters, limits for the formation of cracks in cast microstructures in BTR I have been derived. The current joint research project between VAI and CDL-MCC will continue with a focus on higher carbon steels and the influence of alloying, microalloying and tramp elements.
For BTR II the joint development of the in-situ materials characterization test between VAI and the University of Leoben has yielded first novel results for Nb alloyed steel. Although – at the present state of development – some restrictions with respect to temperature control and maximum tensile forces exist, the method is adequate for material characterization in the BTR II fully featuring the continuously cast material properties. For the immediate future, the work will focus on a further optimization of the testing conditions and an improvement in the reproducibility of the test results.

ACKNOWLEDGEMENTS

The project described here is funded by VAI and the Christian Doppler Research Society.

REFERENCES

[1] Matsumiya, T., M. Ito, H. Kajioka, S. Yamaguchi and Y. Nakamura: “An evaluation of critical strain for internal crack formation in continuously cast slabs”, Trans. Iron Steel Inst. Jpn. Vol. 26, (1986), 6, pp. 540-545

[2] Miyazaki, J., T. Mori and K. Narita: ”Influence of deformation on the internal crack formation in continuously cast bloom”, Continuous Casting of Steel, Second Process Technology Conference, Chicago, Vol. 2 (1981), pp. 35-43

[3] Wünnenberg, K. and R. Flender: „Investigation of internal crack formation in continuous casting, using a hot model“, Iron and steelmaking, Vol 12, (1985), 1, pp. 22-29

[4] Won, Y. M., T.- J. Yeo, D. J. Seol and K. H. Oh: “A new criterion for internal crack formation in continuously cast steels”, Metallurgical and Materials Transactions B, 31 (2000), pp. 779-794

[5] Xia, G., J. Zirngast, H. Hiebler and M. Wolf: Proc. 1st Conference on Continuous Casting of Steel in Developing Countries, The Chinese Society for Metals, Beijing (1993), pp. 200-210

[6] Hiebler, H. and Bernhard, C: Publ. Univ. of Miskolc (Hungary), Series B, Metallurgy, Vol. 39, (1995), 1, pp. 363-372

[7] Hiebler, H., J. Zirngast, C. Bernhard and M. Wolf: Proc. Steelmaking Conference, Vol. 77, (1994), pp. 405-416

[8] Bernhard, C, H. Hiebler and M.M. Wolf: Proc. Conf. on Continuous Casting of Steel in Developing Countries, The Chinese Society for Metals, Wuhan (1997), pp. 224-229

[9] Hiebler, H. and Ch. Bernhard: “Mechanical Properties and Crack Susceptibility of Steel during Solidification”, steel research Vol. 69 (1999), 8+9, pp. 349-355

[10] Bernhard, Ch, H. Hiebler and M. Wolf: “Simulation of Shell Strength Properties by the SSCT Test”, Trans. ISIJ 36 (1996), Supplement, pp. 163-166

[11] Diener, A., A. Drastik and K. Rüttiger: Casting and solidification of steel III, VDEh, ECSC 7210-CA/112, Brussels (1982)

CURRICULUM VITAE

Christian Bernhard completed his master's degree in Metallurgy at Leoben University for Mining, Metallurgy and Materials in 1994, and his Ph.D. in 1998 in the field of continuous casting at the Institute of Ferrous Metallurgy. After gaining his doctorate, he continued in his position as lecturer and researcher on continuous casting at Leoben University. In 2002 he became head of the Christian Doppler - laboratory for Metallurgical Fundamentals of Continuous Casting Processes.